Inorg. Chem. **2002**, *41*, 4624–4626

Synthesis, Structure, Properties, and Phosphatase-Like Activity of the First Heterodinuclear $Fe^{III}Mn^{II}$ Complex with the Unsymmetric Ligand H_2BPBPMP as a Model for the PAP in Sweet Potato

Peter Karsten,[1a] Ademir Neves,*[,1a] Adailton J. Bortoluzzi,[1a] Mauricio Lanznaster,[1a] and Valderes Drago[1b]

Departamento de Química and Departamento de Física, Universidade Federal de Santa Catarina, Campus Trindade, BR-88040-900 Florianópolis—SC, Brazil

Received April 26, 2002

The new heterodinuclear mixed valence complex $[Fe^{III}Mn^{II}(BPBPMP)(OAc)_2]ClO_4$ (**1**) with the unsymmetrical N_5O_2 donor ligand 2-bis[{(2-pyridylmethyl)-aminomethyl}-6-{(2-hydroxybenzyl)-(2-pyridylmethyl)}-aminomethyl]-4-methylphenol (H_2BPBPMP) has been synthesized and characterized. Compound **1** crystallizes in the monoclinic system, space group $P2_1/c$, and has an $Fe^{III}Mn^{II}$-(μ-phenoxo)-bis(μ-carboxylato) core. Two quasireversible electron transfers at –870 and +440 mV versus Fc/Fc^+ corresponding to the $Fe^{II}Mn^{II}/Fe^{III}Mn^{II}$ and $Fe^{III}Mn^{II}/Fe^{III}Mn^{III}$ couples, respectively, appear in the cyclic voltammogram. The dinuclear $Fe^{III}Mn^{II}$ center has weakly antiferromagnetic coupling with $J = -6.8$ cm^{-1} and $g = 1.93$. The ^{57}Fe Mössbauer spectrum exhibits a single doublet, $\delta = 0.48$ mm s^{-1} and $\Delta E_Q = 1.04$ mm s^{-1} for the high spin Fe^{III} ion. Phosphatase-like activity at pH 6.7 with the substrate 2,4-bis(dinitrophenyl)phosphate reveals saturation kinetics with the following Michaelis–Menten constants: $K_m = 2.103$ mM, $V_{max} = 1.803 \times 10^{-5}$ mM s^{-1}, and $k_{cat} = 4.51 \times 10^{-4}$ s^{-1}.

Purple acid phosphatases (PAP) include a family of dinuclear metal-containing enzymes, which are able to catalyze the hydrolysis of a great range of activated phosphoric acid esters and anhydrides. Their optimum catalytic activities occur in the pH range between 4 and 7. Purple acid phosphatases have been isolated in animals, plants, and fungi.[2] The mammalian PAP uteroferrin from a porcine uterus with a dinuclear $Fe^{III}Fe^{II}$ center is well characterized.[3] The red kidney bean purple acid phosphatase is the best described plant enzyme, which comprises an $Fe^{III}Zn^{II}$ center.[4]

In sweet potato, a PAP with a dinuclear $Fe^{III}Mn^{II}$ center has been previously described,[5,6] and more recently, an isoform of it with an $Fe^{III}Zn^{II}$ core[7] has been isolated.

Preparing and characterizing a low molecular weight inorganic analogue that mimics the properties of this enzyme was the aim of this bioinorganic chemistry study. Only a few heterodimetallic compounds which contain an $Fe^{III}Mn^{II}$ center have been synthesized and characterized.[8−10]

In this work, we present as a model for the PAP of sweet potato the structure, physical properties, and phosphatase-like reaction with the activated substrate 2,4-bis(dinitrophenyl)phosphate of the complex $[Fe^{III}Mn^{II}(BPBPMP)(OAc)_2]ClO_4$ (**1**) with the unsymmetrical ligand 2-bis[{(2-pyridylmethyl)-aminomethyl}-6-{(2-hydroxybenzyl)(2-pyridylmethyl)}-aminomethyl]-4-methylphenol (H_2BPBPMP). It should be noted that the ligand H_2BPBPMP comprises only one terminal phenolate and therefore is capable of stabilizing mixed valence species.

The preparation of H_2BPBPMP is shown in Figure 1.

Complex **1** was prepared by simultaneously adding methanolic solutions of $Mn(OAc)_2 \cdot 6H_2O$ (0.2 mmol) and $FeCl_2 \cdot 4H_2O$ (0.2 mmol) to a methanolic solution containing the ligand 2-bis[{(2-pyridylmethyl)-aminomethyl}-6-{(2-hydroxybenzyl)(2-pyridylmethyl)}-aminomethyl]-4-methylphenol (H_2BPBPMP) (0.2 mmol) and $NaClO_4$ (0.2 mmol) with magnetic stirring at 40 °C for 30 min to yield a dark violet solution. After the solution was left to stand for a few days at room temperature, a crystalline solid was isolated. Yield: 140 mg, 80%. Anal. Calcd for $C_{38}H_{39}N_5O_{10}ClFeMn$, $M_r = 871.99$: C, 52.34; H, 4.51; N, 8.03. Found: C, 51.55; H,

* To whom correspondence should be addressed. E-mail: ademir@qmc.ufsc.br.

(1) (a) Departamento de Química. (b) Departamento de Física.
(2) Klabunde, T.; Krebs, B. *Struct. Bonding (Berlin)* **1997**, *89*, 177.
(3) Guddat, L. W.; McAlpine, A. S.; Hume, D.; Hamilton, S.; de Jersey, J.; Martin, J. L. *Structure* **1999**, *7*, 757.
(4) Klabunde, T.; Sträter, N.; Fröhlich, R.; Witzel, H.; Krebs, B. *J. Mol. Biol.* **1996**, *259*, 737.
(5) Schenk, G.; Boutchard, C. L.; Carrington, L. E.; Noble, C. J.; Moubaraki, B.; Murray, K. S.; de Jersey, J.; Hanson, G. R.; Hamilton, S. *J. Biol. Chem.* **2001**, *276*, 19084.
(6) Schenk, G.; Ge, Y.; Carrington, L. E.; Wynne, C. J.; Searle, I. R.; Carrroll, B. J.; Hamilton, S.; de Jersey, J. *Arch. Biochem. Biophys.* **1999**, *370*, 183.
(7) Durmus, A.; Eicken, C.; Sift, B. H.; Kratel, A.; Kappl, R.; Hüttermann, J.; Krebs, B. *Eur. J. Biochem.* **1999**, *260*, 709.
(8) Buchanan, R. M.; Mashuta, M. S.; Richardson, J. F.; Oberhausen, K. J.; Hendrickson, D. N.; Webb, R. J.; Nanny, M. A. *Inorg. Chem.* **1990**, *29*, 1301.
(9) Holman, T. R.; Wang, Z.; Hendrich, M. P.; Que, R., Jr. *Inorg. Chem.* **1995**, *34*, 134.
(10) Dutta, S. K.; Werner, R.; Flörke, U.; Mohanta, S.; Nanda, K. K.; Haase, W.; Nag, K. *Inorg. Chem.* **1996**, *35*, 2292.

10.1021/ic025674k CCC: $22.00
Published on Web 08/06/2002

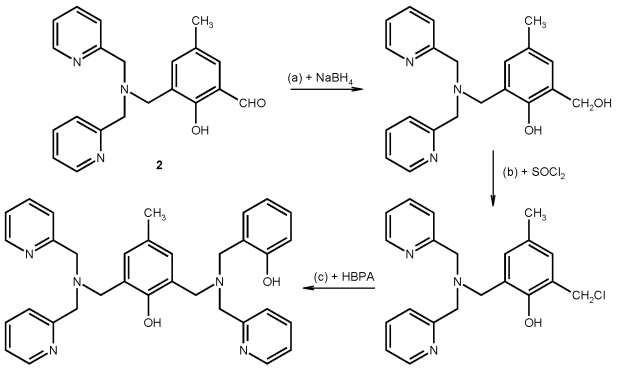

Figure 1. 3-[(Bis-pyridin-2-ylmethyl-amino)-methyl]-2-hydroxy-5-methyl-benzaldehyde[11] (**2**) was reduced with $NaBH_4$ (a) and followed by the reaction with $SOCl_2$ (b). The nucleophilic substitution of the chloride with (2-hydroxybenzyl)(2-pyridylmethyl)amine[15] (HBPA) (c) results in the unsymmetrical ligand.

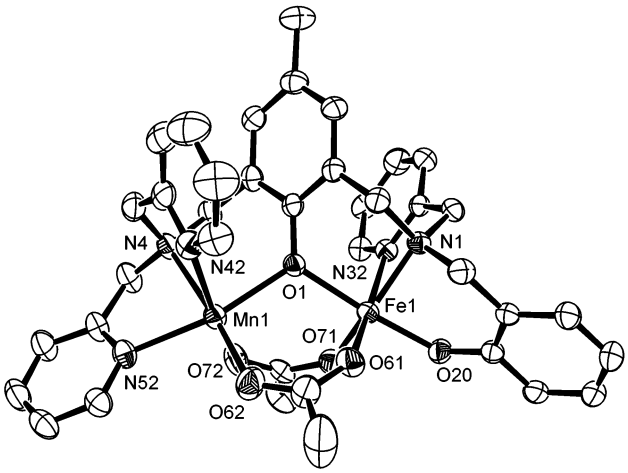

Figure 2. ORTEP plot (50% probability) of the cation of **1**. Selected bond lengths (Å) and angle (deg): Fe1−O1 2.010(2), Fe1−O20 1.882(2), Fe1−O61 2.037(3), Fe1−O71 1.974(3), Fe1−N1 2.215(3), Fe1−N32 2.181(3), Mn1−O1 2.155(2), Mn1−O62 2.089(3), Mn1−O72 2.178(3), Mn1−N4 2.279(3), Mn1−N42 2.285(4), Mn1−N52 2.248(3), Fe1···Mn1 3.510(9), Fe1−O1−Mn1 114.86(12).

4.49; N, 7.73. IR, COO region: ν_{as}, 1598 cm^{-1}; ν_s 1414 cm^{-1}.

CAUTION! Perchlorate salts of metal complexes are potentially explosive and therefore should be prepared in small quantities.

Complex **1** (Figure 2) consists of discrete cations, perchlorate anions, and 0.3 water molecules of crystallization. The two metal atoms are bridged by the phenolate oxygen O1 and two carboxylate groups of the acetate ligands.[12]

The two nitrogen atoms N1 and N32, from the tertiary amine and the pyridine group, and the O20 oxygen of the terminal phenolate complete the N_2O_4 coordination sphere of Fe1. The N_3O_3 octahedral coordination sphere of Mn1 is complemented by the three nitrogen atoms N4, N42, and N52, of the bis(2-pyridylmethyl)amine branch. The distances from the nitrogen atoms to Mn1 are rather similar: 2.279(3) Å versus 2.285(4) Å versus 2.248(3) Å.

The average bond lengths around the two metal ions are significantly different, as expected for a heterodinuclear mixed valence species: those around Fe1 average 2.050 Å while those around Mn1 average 2.206 Å. The most obvious differences are found in the distances from the two metal ions to the bridging phenolate oxygen: Fe1−O1 2.010(2) Å versus Mn1−O1 2.155(2) Å. It is worth noting that the two bridging carboxylate groups are bonded asymmetrically to the metal ions. The two M−O bonds in the trans position to the tertiary amines are significantly shorter than the two others.

The observed Fe1···Mn1 distance is 3.510(9) Å, and the angle between Fe1−O1−Mn1 is 114.86(12)°.

Because of the identical $S = {}^5/_2$ spin configuration, the distances of the $Fe^{III}Fe^{II}$ [13] and $Mn^{III}Mn^{II}$ [14] analogues have been drawn on to distinguish the positions assigned to the Fe^{III} and Mn^{II} ions (Table 1).

The electronic spectra of **1** show a broad band centered at 544 nm (ϵ = 2680 L mol^{-1} cm^{-1}), which can be attributed to the phenolate-to-Fe^{III} charge-transfer transition. The PAP in sweet potato shows a tyrosine-to-Fe^{III} charge-transfer transition at 560 nm (ϵ = 3200 L mol^{-1} cm^{-1}).[6] No intervalence charge-transfer band can be observed in the near-IR region for complex **1**.

The cyclic voltammogram (Figure S1) of **1** reveals two quasireversible redox processes corresponding to successive one-electron-transfer steps. The redox steps at −870 and + 440 mV versus Fc/Fc^+ correspond to the $Fe^{II}Mn^{II}/Fe^{III}Mn^{II}$ and $Fe^{III}Mn^{II}/Fe^{III}Mn^{III}$ couples, respectively. These values are in close agreement with the first and last redox steps observed for the Fe_2[15] and Mn_2[14] homologues, respectively (Table 2).

With the comproportionation reaction and its equilibrium constant K_{com}, the stability of the mixed valence species can be quantified:

Table 1. Structural Comparison of Complex **1** with Its Iron and Manganese Analogues[a]

compound	M^{III}−O1	M^{II}−O1	M^{III}−O20	M···M	M−O−M
$[Fe^{III}Mn^{II}(L1)(OAc)_2]^+$	2.010	2.155	1.882	3.551	114.86
$[Mn^{III}Mn^{II}(L1)(OAc)_2]^+$	1.9275	2.179	1.852	3.497	116.61
$[Fe^{III}Fe^{II}(L1)(OAc)_2]^+$	2.005	2.102	1.902	3.5041	117.14

[a] Distances reported in angstroms; angles reported in degrees. $(BPBPMP)^{2-} = (L1)^{2-}$.

Table 2. Cyclovoltammetric Data for the $[M^{III}M^{II}(L1)(OAc)_2]^+$ Complexes[a]

compound	$E_{1/2}(1)$, mV	$E_{1/2}(2)$, mV	$\Delta E_{1/2}$, mV
$[Fe^{III}Mn^{II}(L1)(OAc)_2]^+$	−870	+440	1310
$[Mn^{III}Mn^{II}(L1)(OAc)_2]^+$	−445	+520	965
$[Fe^{III}Fe^{II}(L1)(OAc)_2]^+$	−890	−20	870

[a] Scan rate 100mV/s in acetonitrile, versus ferrocene. $\Delta E_{1/2} = |E_{1/2}(1) - E_{1/2}(2)|$. $(BPBPMP)^{2-} = (L1)^{2-}$.

(11) Uozumi, S.; Furutachi, H.; Ohba, M.; Okawa, H.; Fenton, D. E.; Shindo, K.; Murata, S.; Kitko, D. J. *Inorg. Chem.* **1998**, *37*, 6281.
(12) Space group: monoclinic, $P2_1/c$, a = 19.513(3) Å, b = 10.7500(18) Å, c = 20.908(7) Å, α = 90°, β = 117.197(14)°, γ = 90°, V = 3900.9(16) $Å^3$, Z = 4. $F(000)$ = 1800. Absorption coefficient = 0.828 mm^{-1}. Wavelength = 0.71073 Å, T = 208.(2) K, data/restraints/parameters 5654/0/512. Final R indices [$I > 2\sigma_I$], R1 = 0.0352, wR2 = 0.0871. Largest diff. peak and hole, 0.997 and −0.466 e·$Å^{-3}$.
(13) Neves, A.; Horn, A.; Lanznaster, M.; Vencato, I.; Bortoluzzi, A. Manuscript in preparation.
(14) Karsten, P.; Neves, A.; Bortoluzzi, A. J.; Strähle, J.; Maichle-Mössmer, C. *Inorg. Chem. Commun.* **2002**, *5*, 434.
(15) Neves, A.; de Brito, M. A.; Drago, V.; Griesar, K.; Haase, W. *Inorg. Chim. Acta* **1995**, *237*, 131.

$$[M^{II}{}_2(BPBPMP)(OAc)_2] + [M^{III}{}_2(BPBPMP)(OAc)_2]^{2+} \leftrightarrows 2[M^{III}M^{II}(BPBPMP)(OAc)_2]^{+}$$

and

$$\Delta E_{1/2} = (RT/nF)\ln K_{com}$$

This confirms that the heteronuclear mixed valence species $[Fe^{III}Mn^{II}(BPBPMP)(OAc)_2]^+$ is more stable than its homonuclear iron and manganese analogues.

The measurement of the magnetic moment between 5 and 300 K in complex **1** reveals a weak antiferromagnetic coupling of the dinuclear $Fe^{III}Mn^{II}$ center (Figure 3). The magnetic moment at 300 K amounts to $\mu_{eff} = 7.39\ \mu_B$ per dinuclear center and drops to $\mu_{eff} = 0.86\ \mu_B$ at 5 K per dinuclear center. Susceptibility data were least-squares fitted by using the Hamiltonian for an isotropic exchange interaction, $H = -2JS_1S_2$ (S_1 and $S_2 = {}^5/_2$). The exchange-coupling constant J was determined as $-6.8\ cm^{-1}$, and $g = 1.93$.

Compared with the enzyme, the antiferromagnetic coupling is very low ($-6.8\ cm^{-1}$ vs $> -70\ cm^{-1}$).[2] This may be due to the presence of an μ-oxo bridge in the enzyme in contrast to a μ-phenolate bridge in complex **1**. Furthermore, the Fe^{III}—Mn^{II} internuclear distance in the enzyme is significantly shorter (2.9 Å in the PAP vs 3.5 Å in **1**).[16]

The presence of a high spin Fe^{III} ion in **1** has been confirmed, in addition to the crystal structure and the measurement of the magnetic moment, by a ^{57}Fe Mössbauer spectrum at 80 K, which shows a single quadrupole-split doublet with a quadrupole splitting of $\Delta E_Q = 1.04\ mm\ s^{-1}$ and an isomer shift of $\delta = 0.48\ mm\ s^{-1}$ versus iron foil.[17]

Experiments to examine the phosphatase-like activity have been carried out with the activated substrate 2,4-bis(dinitrophenyl)phosphate[18] and by monitoring the concentration of the liberated 2,4-dinitrophenolate anion with UV spectroscopy (calculation of the concentration with the aid of the absorbance of the 2,4-dinitrophenolate anion at 400 nm with $\epsilon = 19100\ L\ mol^{-1}\ cm^{-1}$).

To take into account the autohydrolysis of the substrate, the reference cuvette cell contained the same substrate concentration under the same conditions ($T = 25$ °C, ionic strength adjusted to 0.1 M $LiClO_4$, solvent H_2O/CH_3CN, 1:1) as the sample cuvette cell (complex concentration 4×10^{-4} M).

In the first experiment, the pH dependency of the catalytic activity between 3.63 and 8.53 was determined (pH 3.63−7.12 buffer MES 25 mM, pH 7.15−8.53 buffer HEPES 25 mM). The curve of the catalytic activity of **1** reveals a maximum efficiency at about pH 6.7. Sigmoidal fits to the curve reveal two pK_a's, 5.80 ± 0.02 and 7.76 ± 0. These results suggest that the variation in the speed of the catalytic reaction depends on the deprotonation of the coordinated water molecule of the catalytically active species.

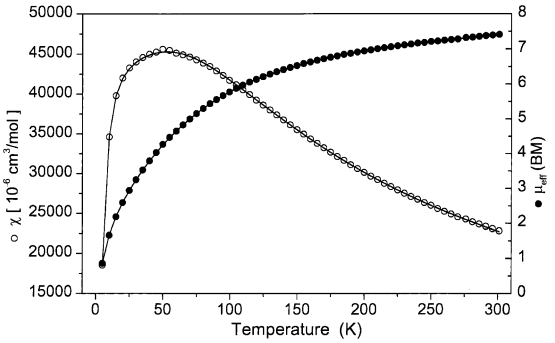

Figure 3. Temperature dependency of the susceptibility χ and the magnetic moment μ_{eff} of complex **1**.

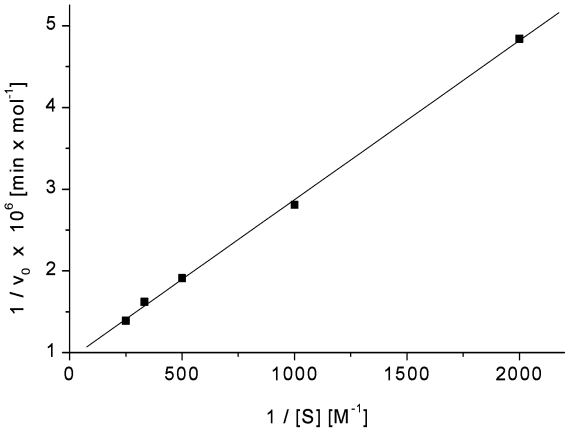

Figure 4. Lineweaver−Burke plot with $K_m = 2.103$ mM and $V_{max} = 1.803 \times 10^{-5}$ mM s^{-1} of the H_2O_2 saturation kinetics for **1** at pH 6.7.[19]

The determination of the initial rates at pH 6.7 as a function of the concentration of the substrate (0.5−4 mM) reveals saturation kinetics with Michaelis−Menten-like behavior. A linearization after Lineweaver−Burke (Figure 4) gives the following values: $K_m = 2.103$ mM, $V_{max} = 1.803 \times 10^{-5}$ mM s^{-1}, and the catalytic constant $k_{cat} = V_{max}/[\mathbf{1}] = 4.51 \times 10^{-4}\ s^{-1}$. Under these conditions, complex **1** is more than 2.5×10^3 times more effective than the substrate which in the same pH region undergoes autohydrolysis ($k = 1.8 \times 10^{-7}\ s^{-1}$).

The isolation of the catalytically active species to determine its structure and properties and the mechanism of the catalytic cycle is the subject of further research.

Acknowledgment. We thank Dr. Ulrich Ziener from the University of Ulm/Germany for the elemental analysis and Prof. Joachim Strähle from the University of Tübingen/Germany for the measurement of the magnetic properties. Financial support was received from CNPq and PRONEX (Brazil). P.K. is grateful to CNPq Proc. 150136/97-8(NV) (Brazil) for a scholarship in 2002.

Supporting Information Available: Figure S1, showing the cyclic voltammogram of **1**, and X-ray crystallographic details for complex **1** in CIF format. This material is available free of charge via the Internet at http://pubs.acs.org.

IC025674K

(16) Schenk, G.; Carrington, L. E.; Hamilton, S.; de Jersey, J.; Guddat, L. W. *Acta Crystallogr., Sect. D* **1999**, *55*, 2051.
(17) Fluck, E.; Kerler, W.; Neuwirth, W. *Angew. Chem.* **1963**, *75*, 461.
(18) Bunton, C. A.; Farber, S. J. *J. Org. Chem.* **1969**, *34*, 767.
(19) To 2 mL of an aqueous solution of 50 mM MES and 0.2 M $LiClO_4$, which was adjusted to pH 6.7, was added 0.1 mL of a 1.6×10^{-3} M solution of **1** in acetonitrile and between 0.1 and 1.8 mL of a 2.0×10^{-2} M solution of 2,4-bis(dinitro-phenyl)-phosphate in acetonitrile. This solution was completed with acetonitrile to a volume of 4 mL.